RECONSTRUCTING DECAYS OF STAU PARTICLES USING AN ALL SILICON DETECTOR AT THE ILC

A Thesis submitted in Partial Satisfaction
Of the Requirements for the Degree of
Bachelor of Sciences in Physics
at the
University of California, Santa Cruz

By
Dustin Stolp
May 31, 2010

____
Bruce Schumm
Advisor

____
David P. Belanger
Senior Thesis Coordinator

____
David P. Belanger
Chair, Department of Physics

ACKNOWLEDGEMENTS:

I would like to thank Professor Bruce Schumm for his help and guidance during the duration of this project. When I had any questions about the project or the advanced physics involved he thoughtfully answered them all. Also for being available for help when I needed it. The book he wrote was very helpful in beginning to learn about the spectacular world of particle physics. And lastly I want to thank him for having an awesome sense of humor.

I also would like to thank Alex Bogert for his in depth knowledge of the project and writing programs in Java. At the beginning I had no idea how to set all the necessary programs up on my computer and he walked me through the process. He also allowed me to pick his brain many times to find methods and documentation necessary to write the proper code. Finally I would also like to thank him for always being available to answer any of my questions and being an all around good guy.

My girlfriend was very helpful throughout the process. When I would be writing code for what felt like all night, she would bring me food and tea. Also, my parents were helpful in both their encouragement and financial support. I really appreciate that they were interested in my project and were willing to listen to me ramble on about things I barely knew.

Finally I would like to thank the UCSC physics department. I appreciate Professor Howard Haber for answering some questions I had about supersymmetry. I have been impressed with the entire faculty’s’ helpfulness and honesty. Finally, my fellow classmates were a great team to work with throughout the years.

TABLE OF CONTENTS:

ABSTRACT:
At the upcoming International Linear Collider tracking supersymmetric tau particles (staus) and their descendants is necessary to explore possible new physical processes. Some theories to be probed are supersymmetry and the method of supersymmetry breaking. In the Gauge Mediated Supersymmetry Breaking model a meta-stable stau can be the next to lightest supersymmetric particle and produces the lightest supersymmetric particle, the gravitino. Simulating stau decay events requires modifications in tracking methods to maximize the efficiency of reconstructing tracks of the indirect decay products of the stau. This project focused on reconstructing tracks using a silicon tracking detector with sparse tracking layers. The tracking methods adjusted in this project are known as Seed Tracker and Seed Extend Tracker. Applying cuts to Seed Tracker increased the efficiency for tracks that originate further from the collision center. Applying cuts to Seed Extend Tracker increased the total efficiency from 30% to 75%.

THE ILC

The International Linear Collider (ILC) is expected to be built in the next 10 years. Although it does not have a host country yet, research is being done all over the world to develop the best possible design for the accelerator and detector. The ILC will complement the currently running Large Hadron Collider (LHC). The LHC is likely to discover exotic particles if they exist, however the ILC will dissect the process in which these are created and in turn will allow greater understanding of their characteristics. The ILC will collide electrons and positrons at center-of-mass energies near 500GeV using 16,000 pure niobium superconducting accelerator cavities chilled to 2K (1). Unlike the LHC which collides protons in a circular path, the ILC will be linear. Due to the electron's small mass the particle accelerator must be linear as to not lose energy via synchrotron radiation. The collider will be 31km long, however in the second stage of the project, there could be an upgrade to a 50km collider with 1TeV collision energy. Figure 1 shows the macroscopic plans for the collider. A beam pulse will have 20 billion particles and have a cross section of 650x5nm. The electron and positron pulses will collide 14,000 times per second. The collisions will occur inside a detector that will be used to reconstruct the tracks taken by particles. These reconstructed tracks can be analyzed to discern the particles properties. The current design involves two detectors that are interchangeably placed around the collision point.

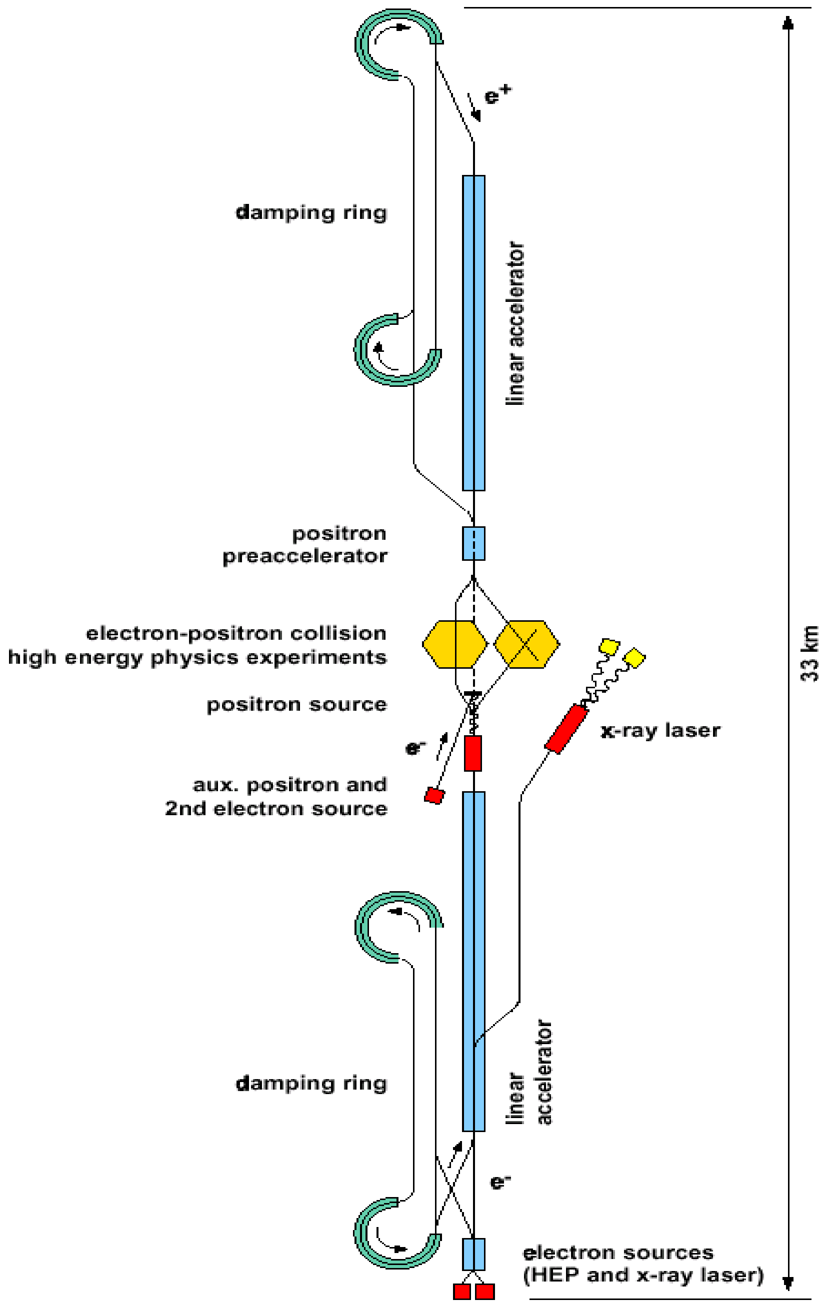

Fig. 1: Macroscopic ILC design. The plans for the ILC accelerators and the position of the collision point are apparent from this design. The two yellow hexagons are the two interchangeable detectors.

THE DETECTORS

In ILC collision events, charged particles will be tracked using detectors. There are currently two detectors being considered; the International Large Detector (ILD), and the Silicon Detector (SiD). Due to the geometry of the detectors, the coordinate system used to give three dimensional locations will be r the radius perpendicular to the beam line, φ the azimuthal angle around the beam line, and z the displacement along the beam line. All the planned detectors will be symmetric in the φ direction. In order from smaller radius to larger radius, all planned detectors will consist of highly pixilated Silicon strip vertex layers, mid range tracking mechanisms, and high precision granulated calorimeters. Surrounding each detector will be a solenoid producing a 4-5T magnetic field in the z direction. The magnitude of the magnetic field is different for each detector design. This magnetic field will allow for calculation of the transverse momentum based on the curvature of the path that the charged particle takes.

The difference between the detectors is largely the method that the tracking section uses to reconstruct tracks. The ILD design uses a gaseous volume inside two plates charged to opposite voltages. As a charged particle goes through the chamber it ionizes atoms in the gas, causing the electron and ion to move in the z direction towards opposite plates, signaling a hit. The benefit of this is it allows for near continuous tracking. Originally there was difficulty in measuring the z component of the track due to the symmetry of the gaseous tracker. However, with the introduction of Time Projection Chambers (TPC), this potential problem was eliminated, and now three dimensional track reconstructions can be made by measuring the time it takes for ionized electrons to reach the plates. Although efforts have been made to limit the wandering of electrons as they drift towards the plates, Brownian motion does occur and produces a hit resolution of order 100μm in r/φ and 1mm in z. One benefit of continuous tracking via TPC is that particles may be identified from measurement of loss of ionization energy (8).

THE SiD

The SiD detector gives the best possible resolution for three dimensional points. This is due to having precise silicon strip detectors. The SiD relies on 10 concentric cylindrical layers. The ends of the cylindrical layers will be capped with particle detection material. The distance from the collision point to the end caps will increase with the radius of the cylinder. Like the other detectors, the first five layers of the SiD are a powerful silicon pixel vertex detector reaching 6.04cm in radius. Beyond the vertex detector there will be five more barrel tracking layers between 21.8cm and 121.8cm radius. Outside of these tracking layers will be a silicon-tungston electromagnetic calorimeter, a highly segmented hadronic calorimeter, and a muon calorimeter followed by a solenoid producing a 5T magnetic field. Figures 2 and 3 show a quarter cross section of the detector and the tracking layers respectively. The use of precise silicon strip sensors in the SiD design provides a two dimensional resolution of 5μm (4).

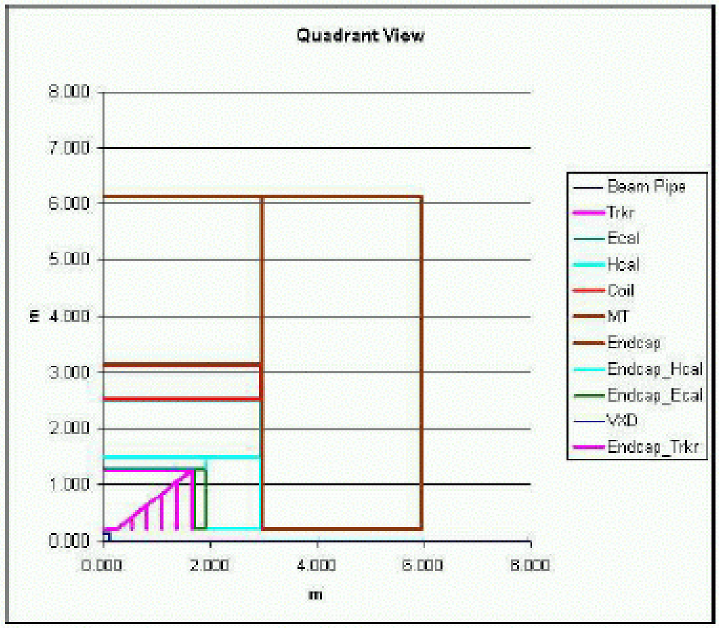

Fig. 2: The SiD design. This shows the geometry of the detector viewed from the r-z plane with the z direction being the horizontal axis. The barrel tracking layer is the larger rectangle in the lower left portion of the graph. The vertex tracking layer is the very small rectangle in the lower left corner. The electromagnetic calorimeter lies directly above the barrel tracking layer (7).

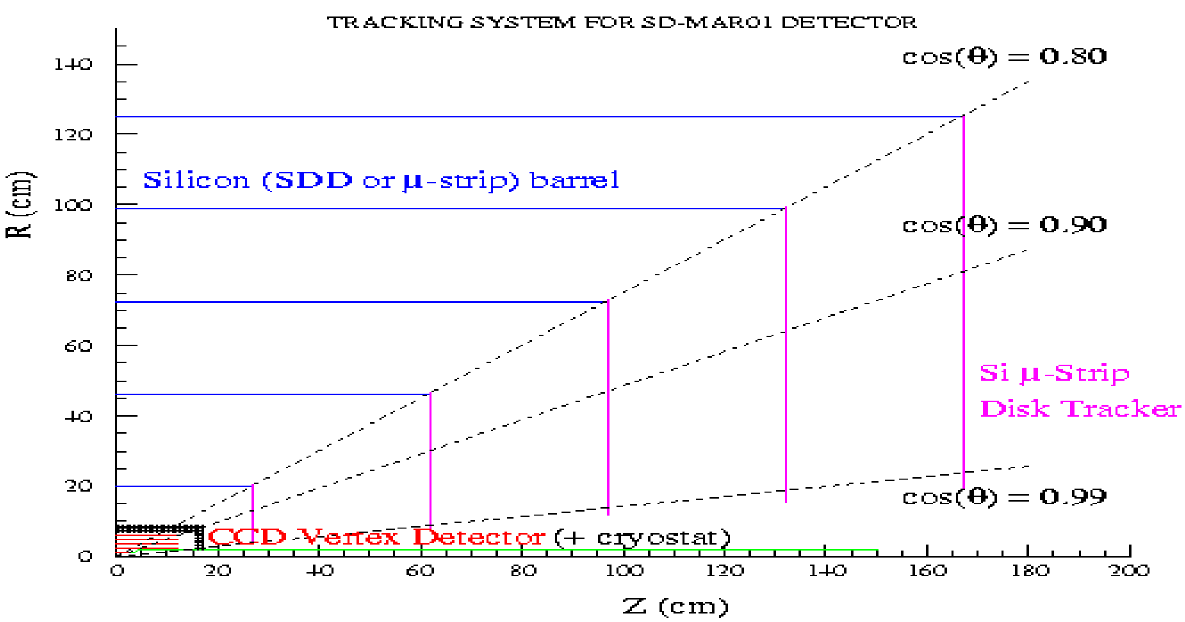

Fig. 3: SiD tracking layers. This can be considered a zooming in of the lower left hand corner of Fig. 2. This graph shows the 5 barrel tracking layers and the smaller vertex tracking layers in the lower left corner (7).

The magnitude of the magnetic field, 5T, is larger in the SiD than in the other designs. During a collision there will be much background to interfere with events of interest. With a larger magnetic field, the background will be forced to smaller radii around the beam line and will not enter the vertex tracking layers. This allows for the placement of the vertex detector to be closer to the collision point. Having a vertex tracker that is closer to the beam line is advantageous because it allows for tracking of promptly decaying particles (8).

Due to the direction of the magnetic field being in the z-direction, each charged particle's track is helical with a circular projection in the r/φ plane. The direction the particle moves around the circle is dependant on the sign of its electromagnetic charge. The magnetic field also helps to measure the transverse momentum of a particle.

$$P_{\perp}c=300Bqr \qquad \text{Eq. 1}$$

In this equation $P_{\perp}$ is the transverse momentum in GeV/c, c is the speed of light in m/s, B is the magnetic field in Tesla, q is the electromagnetic charge of the particle and r is the two dimensional radius in meters of the helix the particle makes as it moves through the detector. Because the SiD has excellent r/φ point resolution, Eq. 1 shows that it also has excellent transverse momentum resolution. Figure 4 compares the transverse momentum resolution of the SiD (marked S) with the ILD (marked L) designs and shows that at higher momentum, the SiD has a superior momentum resolution. However, a particle of lower momentum is not measured with as good a resolution due to the silicon material it moves through. At the ILC, however, most particles of interest will have high momentum. Although the resolution of the SiD is comparable to the other detectors, it has come under question as to whether it can correctly reconstruct mid-range particle decays because of its small number of tracking layers. In a mid-range decay, a parent particle will have a non-prompt track (a track that arises within the barrel tracking layer). Therefore, to prove its validity, it is necessary to prove that it is possible to reconstruct non-prompt tracks using the SiD.

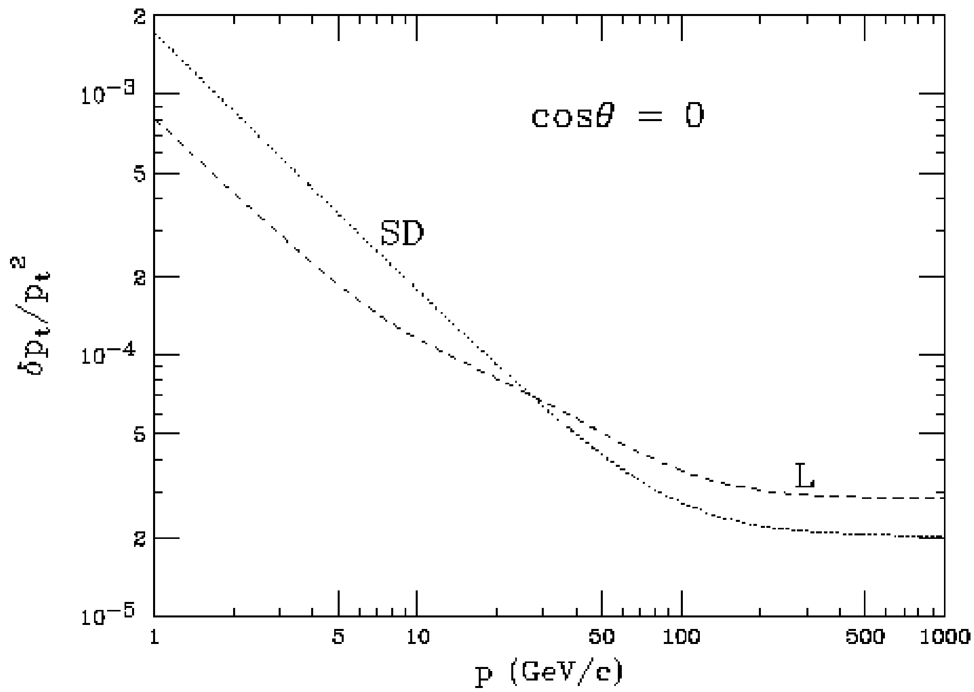

Fig. 4: Transverse momentum resolution of the ILD vs. the SiD. This graph shows the transverse momentum resolution for the SiD (marked S) and the ILD (marked L) designs as a function of a charged particle's transverse momentum. The ILD has better momentum resolution for slower tracks (7).

As particles pass through the SiD they can leave information about their trajectories. The tracking layers are made of semi-conducting silicon strip detectors. A passage of a particle through the detector is signaled if ionization occurs inside the detector. In order for the ionization to take place a charged particle must pass through it. Due to this, the tracking layers can only reconstruct tracks from charged particles. Once the particles hit the highly segmented calorimeter, the pattern of the hits on the calorimeter can provide information about the particle that entered. Also, hadronic particles (particles made of quarks) will create hits in the hadronic calorimeter to signify their hadronicity. Finally, muons make their way through the entire detector, so the outermost layers of the detector will be a muon identification system. If there are particles (such as gravitinos) created that do not leave information in the detector because they are so weakly interactive, their mass and energy can be inferred by finding missing energy in an event.

To prove that the SiD can correctly reconstruct non-prompt tracks, simulations must be done to show how events of interest would occur inside the SiD. Simulating events in the SiD can perfect tracking methods that will be implemented in the actual SiD at the ILC.

SUPERSYMMETRY AT THE ILC

Although the Standard Model does an excellent job of explaining physics involving the electroweak and strong interactions, it is apparent that it has limitations beyond the electroweak scale. According to (6), the

Standard Model will have to be extended to describe physics at higher energies. It seems obvious that new physics exists in the 16 orders of magnitude in energy between the presently explored territory near the electroweak scale, and the scale which gravitational effects become important.

Although the Higgs Boson has yet to be found in a detector, the main argument for the existence of supersymmetry depends on the existence of the Higgs Boson. A problem with the Standard Model is that it allows for disturbing sensitivity of the Higgs potential to new physics in almost any imaginable extension of the Standard Model (6). This limitation of the Standard Model is known as the Hierarchy Problem. To solve this, supersymmetry creates a symmetry in which for every boson particle there is a fermion particle of the same properties and visa versa in order for the quantum corrections to cancel out. This makes supersymmetry an attractive extension to the Standard Model for particle physics.

Currently no supersymmetric particles have been detected, however the energies at which these particles would exist have yet to be fully probed. The effect of supersymmetry is the symmetry of particles between their normal state and their supersymmetric state. The difference in internal angular momentum between the two states is always ½. To differentiate between the two states the supersymmetric counterparts to normal particles are called sparticles. Supersymmetric leptons are called sleptons and supersymmetric quarks are called squarks. The obvious problem with supersymmetry is that it is broken in nature because most of our known universe is made of normal matter. This broken symmetry leads to supersymmetric particles that have more mass than their normal counterparts.

The Standard Model of Particle Physics incorporates the mediating particles of the strong and the electroweak interactions, as well as three generations of matter. Within the three generations of matter there are leptons and quarks. Leptons are particles that are not affected by the strong interaction. The three generations of leptons are electrons (e), muons (μ), taus (τ) and each associated neutrino. Quarks, however, are affected by the strong interaction.

There are many theories as to how supersymmetry is broken. In one theory, "the ordinary gauge interactions are responsible for the appearance of supersymmetry breaking" (6). This theory is called Gauge Mediated Supersymmetry Breaking (GMSB). In GMSB the lightest supersymmetric particle (LSP) is a spin-3/2 gravitino ($g^{\sim}_{3/2}$). This is a supersymmetric partner of a spin-2 graviton (g_2), the theoretical force particle for gravity. The next to lightest superymmetric particle (NLSP) is often “a charged slepton which decays to the corresponding lepton partner and gravitino” (5). Due to cosmological constraints in GMSB, it is likely that the charged slepton NLSP will be a meta-stable supersymmetric tau (“stau” or “$\tau^{\sim}$”). GMSB predicts that the meta-stable stau can decay both promptly and non-promptly. In both cases the stau will decay into a tau and a gravitino (Eq. 2)

$$\tau^{\sim +/-} \rightarrow \tau^{+-} g^{\sim}_{3/2} \qquad \text{Eq. 2}$$

Other than supersymmetry other interesting facets of physics can be probed. As of yet only 5% of the matter in the universe is known, the rest is considered to be dark energy and dark matter. It is believed that dark matter is made up of weakly interacting massive particles (WIMPs). Gravitinos are a dark matter candidate due to their neutral electromagnetic charge and inability to be effected by anything but the weak interaction. Thus the creation of the gravitino at the ILC could lead to more information about the nature of dark matter.

At the ILC it is possible that the electron and positron can annihilate to create a gamma or a Z boson which can then create two oppositely charged staus (Eq. 3 and Fig. 5).

$$e^+e^- \rightarrow \gamma, Z \rightarrow \tau^{\sim +}\tau^{\sim -} \qquad \text{Eq. 3}$$

The taus that the staus produce are very short lived and will not be recognized in the SiD detector. The tau decay will have three decay methods. From the tau branching fraction, there is an 85% probability that the decay will create one stable charged particle. There is a 15% probability that the decay will create three stable charged particles.

Finally it is less than 1% probable that the decay will create five stable charged particles. The charged decay products can be recognized in the SiD detector in the Silicon tracking section as well as the electromagnetic calorimeter. During these decays, the electromagnetic charge of the parent particle and the decay products must remain the same. Thus the signature of a stau event will be the tracks of two meta-stable oppositely charged staus created from the annihilation, which are kinked at the point where the stau and the tau decays.

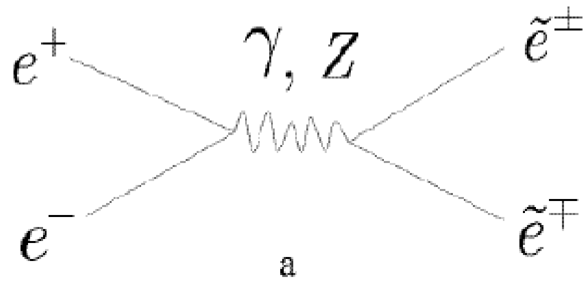

Fig. 5: Slepton production at the ILC. This is the method that staus can be produced at the ILC. The right hand side of the process shows selectrons instead of staus, however because they are both sleptons, they would both be produced the same way(7).

SiD SIMULATIONS

For stau events, the SiD will initially focus on single pronged decays of the stau. It will only see the stau decay into the tau decay products because the tau is too short lived. In order to effectively find the kink where the stau track ends, the tracks of the tau decay products must be efficiently reconstructed. Because they are not the direct product of the stau, the tau decay products are considered the stau descendants.

Events of interest must be simulated inside a virtual SiD first and combined into a data file in order for tracking methods to reconstruct tracks. These event files provide information about both the particle and the hits that that particle makes. At the ILC however, only the hits from each event will be available. Due to this, the event files are used to find tracking methods that only use the hits from each event. By comparing the particles known to be in each event with the tracks made by the tracking methods, one can find the efficiency of reconstructing tracks. This practice of comparing the true particles with the false particle is called Monte Carlo truth recognition. Once the efficiency for reconstructing the tracks is known, one can make changes to the tracking code to improve its effectiveness.

Simulating ILC events inside detectors has been a method for preparing for the actual ILC for many years. Over this time much code for analyzing and tracking events has been made. The main language in the simulations is Java. To run the Java program with the event files, a framework named Jas3 is used.

It is necessary to define the terms that will be used in the rest of this paper so that no confusion takes place. A particle is a singular independent particle that exists in an event, not a group of the same type of particles such as electrons and staus. A track is the path that each particle takes as it moves through the detector and a hit is the information left on a tracking layer by a particle as it creates a track. Due to the helical track and the geometry of the SiD, in order to create a unique track, three hits on separate layers are needed. The track can be extended to a fourth hit to avoid random combinations of the first three hits. Therefore, at least four hits are necessary to create a track.

The three tracking methods are named Seed Tracker, Garfield Tracker, and Seed Extend Tracker. Seed Tracker uses just the tracking layers, however Garfield Tracker and Seed Extend Tracker compare the hits in the outer tracking layers with the hits in the calorimeter. Garfield Tracker is relatively efficient for tracks originating before the second tracking layer, but has difficulty reconstructing tracks that originate beyond that.

Although it was used in this study, its performance was not optimized. When the three methods work together, Seed Tracker can use any hit it needs to create a track. Then, Garfield Tracker uses all the left over hits that had not been used by Seed Tracker. Finally, Seed Extend Tracker tries to reconstruct any tracks using any remaining hits.

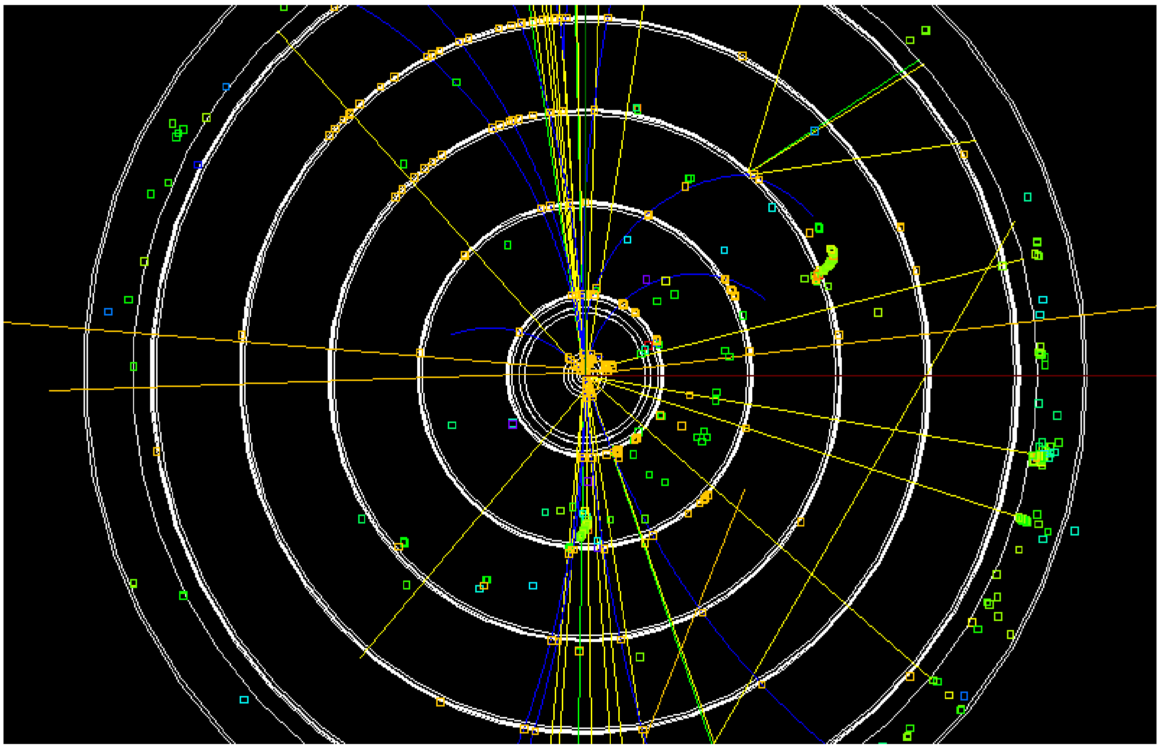

Fig. 6: Projection of an event at the ILC in projected in the r/φ plane. The blue lines are tracks created by charged particles due to the curving of the track. The non charged particle tracks are designated yellow, and the layers are given by the white concentric circles.

TRACKING STAU EVENTS

In order to compare the stau descendant reconstructed tracks with the stau descendant tracks that should be found, one must first create definitions for findable stau descendants. First, one needs to make a list of findable staus so that the descendants of these staus can also be considered findable. Tracks where the particle leaves a hit on the barrel end caps are not considered findable. To get started, we concentrated on tracks of central origin, thus a cut was made to limit |cos (θ)| (where θthe angle between the z-component and the r-component of the momentum) to always being less than 0.7. The descendants from the findable staus must be electromagnetically charged, have a path length that is greater than 45cm, and have a transverse momentum greater than 1 GeV/c in order to be considered findable.

One can then match the particle associated with any reconstructed track with a findable particle. A pure reconstructed track is one in which all the hits that constitute the track come from the same particle. The particle associated with a pure reconstructed track must be a findable particle. However, not all findable particles have their tracks reconstructed. Because an interesting property of each track is the radial origin of the particle, histograms of this property are made of the total number of findable particles and of the number of findable particles that have their tracks reconstructed as a function of radius of origin. Dividing the latter histogram by the former, one can get a graph of the efficiency of reconstructing tracks as a function of radial origin.

SEED TRACKER

The first tracking code that was analyzed is known as Seed Tracker, written by Richard Partridge of SLAC. Seed Tracker uses the ten layers in the vertex and barrel tracking layers as well as barrel end caps to reconstruct tracks. In Seed Tracker, strategies are implemented to find all the possible tracks by using specified combinations of hits. The strategies give three layers in which the hits from these layers are used to define a potential track; the hits from these layers are considered seeds. Because a track can be made by three hits, the strategies find all the combinations of these three hits to create possible tracks. The strategies then extend from these three seeds out to where one would expect a true track to be. The strategies then check to see if there is actually a hit in the region near where the three seed track was extended to, this method is called extend. Finally, the strategy must give one layer in which the extended track has a hit within a small range, this hit location is called confirm. Confirm is similar to extend however it has a tighter cut for the distance between the actual hit and the extended track. Seed Tracker can use multiple strategies, each designating different seed, extend, and confirm layers. Figure 7 shows an example of one strategy.

```
SeedLayer("VertexBarrel", 0, BarrelEndcapFlag.BARREL, SeedType.Extend));
SeedLayer("VertexBarrel", 1, BarrelEndcapFlag.BARREL, SeedType.Seed));
SeedLayer("VertexBarrel", 2, BarrelEndcapFlag.BARREL, SeedType.Seed));
SeedLayer("VertexBarrel", 3, BarrelEndcapFlag.BARREL, SeedType.Seed));
SeedLayer("VertexBarrel", 4, BarrelEndcapFlag.BARREL, SeedType.Confirm));
SeedLayer("TrackerBarrel", 0, BarrelEndcapFlag.BARREL, SeedType.Extend));
SeedLayer("TrackerBarrel", 1, BarrelEndcapFlag.BARREL, SeedType.Extend));
SeedLayer("TrackerBarrel", 2, BarrelEndcapFlag.BARREL, SeedType.Extend));
SeedLayer("TrackerBarrel", 3, BarrelEndcapFlag.BARREL, SeedType.Extend));
SeedLayer("TrackerBarrel", 4, BarrelEndcapFlag.BARREL, SeedType.Extend));
```

Fig. 7: An example strategy. The method of designing a strategy and designating each layer either seed, extend or confirm is shown in this figure. This example designates the second third and fourth vertex layers to be seed, the fifth vertex layer to be confirm, and the rest to be extend. The layer number is signified by the numbers 0-5 and the type of tracking layer is given either VertexBarrel or TrackerBarrel.

Seed Tracker does not attempt to reconstruct tracks of non-promptly decaying particles. In order for Seed Tracker to reconstruct tracks, it requires that tracks extrapolate back to the origin. Because tracks that originate near the origin have a better chance of extrapolating back to the origin, Seed Tracker is very efficient for prompt tracks. However, the efficiency falls off quickly for tracks that originate at higher radii.

Originally there was one default strategy that was used by Seed Tracker. There were two files that contained lists of strategies that worked well together but were not implemented in the original default strategy. These strategies were added to the default strategy to form a default strategy list. A group of strategies that would make the inner layers seeds and extend outward were added to the default strategy list as well. Another group of strategies were added that would make the outer layers seeds and extend inward.

It was once thought possible that some of the descendants were decaying at large angles from the original stau making the stau descendant not findable because they would go through the tracker at an odd angle. A graph was made to find the distribution of cos(β) where β is the angle between the original stau and the stau descendant. This graph is presented in Fig. 8. From this histogram, another cut was made for the definition of a findable stau descendant. The descendant must also have a cos(β) greater than 0.7.

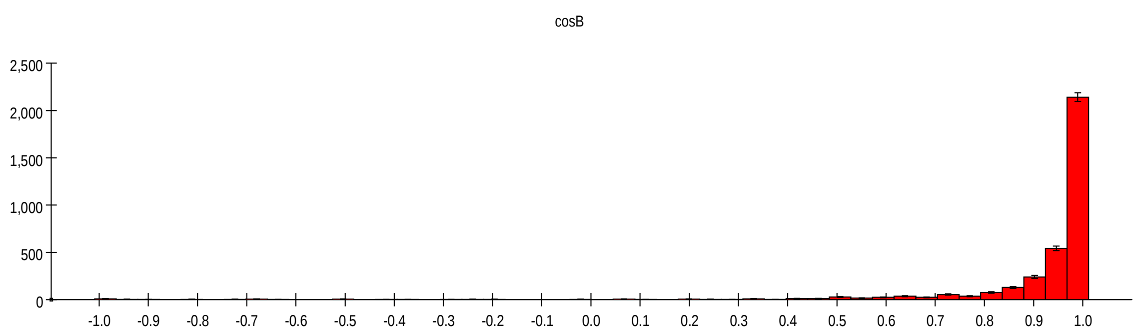

Fig. 8: Cos(β) histogram. In this histogram the x axis shows the cos(β) and the y axis shows the number of instances where cos(β) was within the range in the x axis. From this histogram the cut on cos(β) for findable tracks was made.

SEED EXTEND

Seed Extend Tracker (Seed Extend) is similar to Garfield Tracker in that it uses the electromagnetic calorimeter in track reconstruction. Seed Extend is a method that was created by Chris Mayer and Tyler Rice here at the UCSC physics department. Seed Extend makes all possible tracks using combinations of three hits from the outer four tracking layers. The tracks that are made from these three or more hits are called seeds. Because many of these seeds are fake, cuts are made to obtain a list of seeds called reasonable seeds. One cut is made to control the curvature (1/r where r is the same as Eq. 1) to keep the magnitude of the transverse momentum of reasonable seeds to more than 0.5 GeV/c. There is also a cut made so that the distance of closest approach to the collision point that the circular path makes is less than 200mm. This cut ensures that the ancestors of the seed's particle have large momentum in the radial direction. This is a tight cut to make so far away from the origin. Figure 9 shows the distance of closest approach for all the possible seeds. The cut was increased from 20cm to 30cm to label more seeds as reasonable seeds. An increase in the number of reasonable seeds also increases the number of seeds that are not real.

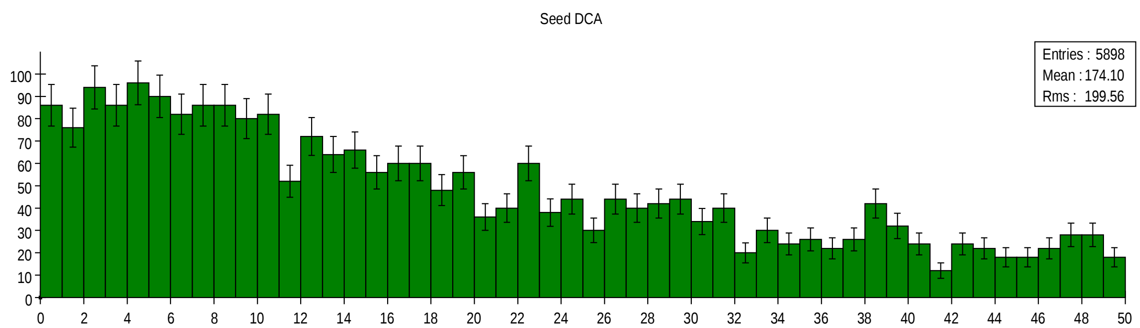

Fig. 9: Seed DCA histogram. This histogram shows the distance of closest approach of all the seeds made by the possible configurations of the hits in the outer layers of the barrel tracking section. The values on the x axis are in cm.

After reasonable seeds are made, they are compared and connected to the hits in the electromagnetic calorimeter. The hits that are made in the electromagnetic calorimeter are grouped together to create a calorimeter track called a stub. The point where the seed connects to the calorimeter is compared to the base of the stub. The original cut for the base difference cut (r/φ offset between the base of the stub and the top of the seed) was 2 mm. The original cut for the z distance between the stub base and the seed top was 200mm. Another cut is made limiting the angle between the seed and the stub to 0.1 radians. This cut is called the base φ difference cut. The base cut is less than the base z cut because the resolution of measuring the two dimensional r/φ position is much greater than the resolution of measuring the z position. Finally, there is also a cut limiting the ratio of the curvature of the seed to the curvature of the stub to less than 10. In cases where there are two stubs that are within these cuts from a reasonable seed, the seed will be extrapolated to the stub with the smallest associated base φ difference. These four cuts are all that transform a list of reasonable seeds into a list of Seed Extend tracks. By modifying these cuts one can change the overall efficiency of Seed Extend track reconstruction.

Due to the design of the SiD there is a certain radial window where the kinks that occur from the decay of meta-stable particles have the highest probability of being reconstructed. This window is between the first and the second barrel tracking layers (218-468mm). This window allows for excellent tracking because seeds that begin here can have hits on all four layers between it and the calorimeter. The next best tracking window is between the second and the third barrel tracking layers (468-718mm). In this range, hits are made on three layers and the calorimeter. Originally it was believed that these regions would also give good efficiency for reconstructing tracks using Seed Tracker.

The window that produces the highest efficiency for reconstructing tracks was the first region analyzed. Histograms were made of the base difference, the base φ difference, the base z difference, and the curvature ratio for all the good seeds of stau descendants that begin in this range and its nearest stub. Figure 10 shows the histogram for the base distance to the nearest stub for stau descendant seeds. The information in Fig. 10 shows that stau descendant seeds are largely within 2mm radial distance from their stubs. However, Fig. 10 also shows that seeds can still be as far as 20mm from its stub. After more suitable cuts were chosen from the information provided by Fig. 10 and the rest of the original histograms, the same histograms were made for particles that begin between the second and third barrel tracking layers. Figure 11 is the same histogram as Fig. 10 for particles that originate between the second and third barrel tracking layers. The new cuts were then modified to include information from the second set of histograms.

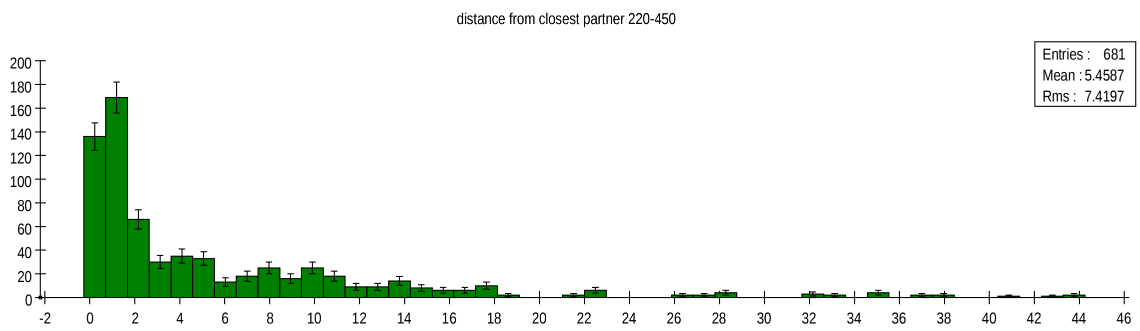

Fig. 10: Base difference between the seed and stub of a findable particle originating between the first and second barrel tracking layers. The values on the x axis are measured in mm.

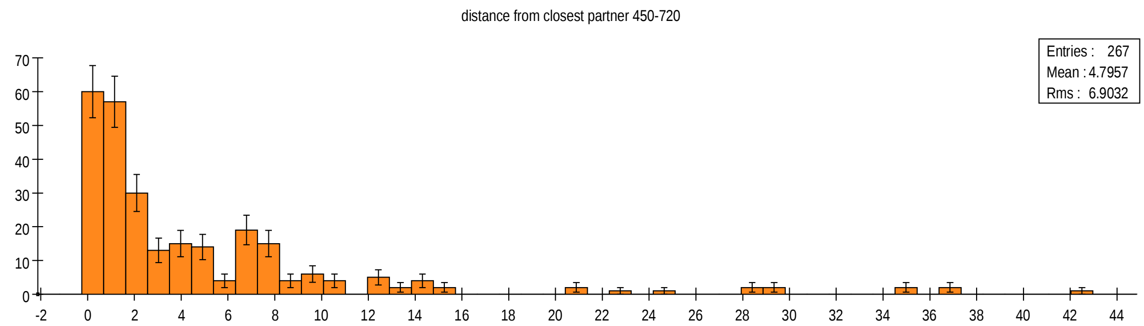

Fig. 11: Base difference between the seed and stub of a findable particle originating between the second and third barrel tracking layers. The values on the x axis are measured in mm.

It is important to realize that although the relaxation of the cuts can allow for more reconstructions of findable stau descendant tracks, it also increases the number of fake tracks that are considered by Seed Extend as real. The fake tracks are made of seeds that are not pure. Because these fake tracks are not created by an underlying particle, they will not have a nearby stub. As can be seen in Fig. 12 the relationship between the fake seed and its connected stub are uncorrelated. There is an ideal location of the cuts so that they increase the efficiency without overly increasing the number of reconstructed fake tracks. Therefore the final cuts made for the relationships between the seed and its stub were 6mm for the base difference, unmodified 200mm for the base z difference, 1 radian for the base φ difference and 40 for the curvature ratio. These cuts were the final cuts that were used to find the overall efficiency of Seed Extend.

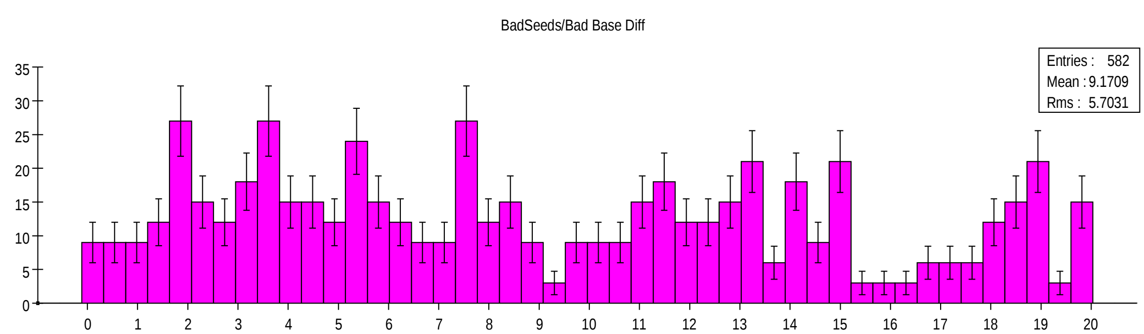

Fig. 12: Base diff of fake tracks created by Seed Extend. This histogram shows the number of fake tracks within a base r difference noted on the x axis. The values on the x axis are in mm.

RESULTS

Stau tracks originate at the origin due to the annihilation of the electron and positron. They will then travel through the detection layers until they decay. At this kink point, the stau descendants originate and continue through the detector. Thus, by taking the difference between the origin and the kink point as defined by the stau descendants, one can reconstruct a stau track. It is therefore necessary to obtain the efficiency for reconstructing stau descendant tracks as a function of radius of origin.

To begin with, the efficiency for reconstructing tracks using Seed Tracker will be analyzed.

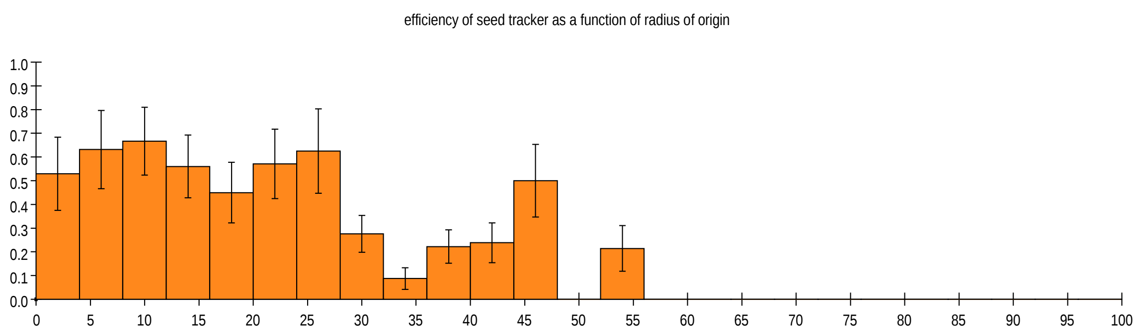

Fig. 13: Previous Seed Tracker efficiency histogram. This is the histogram of the original efficiency of reconstructing tracks using Seed Tracker as a function of the origin of the stau descendant. The values on the x axis are measured in mm.

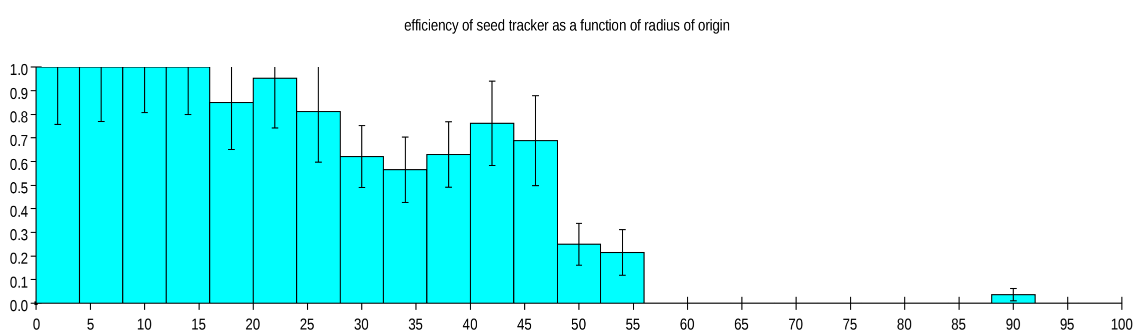

Fig. 14: Updated Seed Tracker efficiency histogram. This histogram is the efficiency of reconstructing stau descendant tracks using original modifications to Seed Tracker as a function of origin of the stau descendant. The original modifications made were on cos(β) and the original addition to the default strategy list. The values on the x axis are measured in mm.

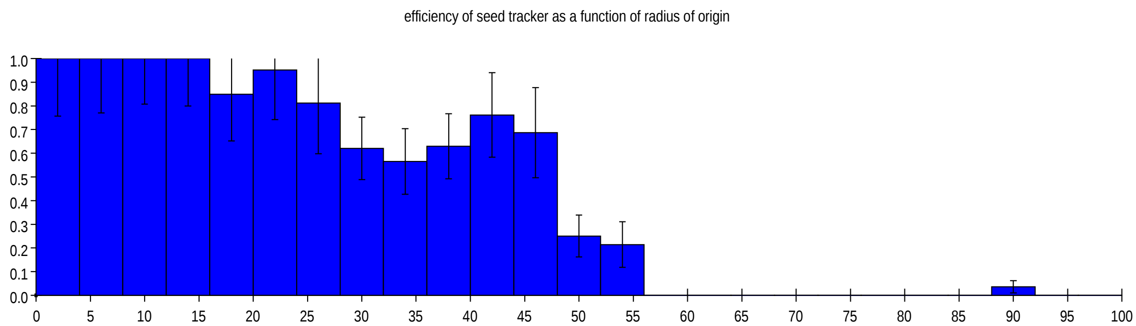

Fig. 15: Further updated Seed Tracker efficiency histogram. This histogram is the efficiency of reconstructing stau descendant tracks using expanded modifications to Seed Tracker as a function of origin of the stau descendant. The modifications to the original Seed Extend to make this histogram were the same modifications used to make Fig. 14, however more strategies were added to the default strategy list beyond the original addition. The values on the x axis are measured in mm.

Comparing Fig. 13 and 14 it is obvious that the addition of more strategies to the default strategy list greatly increased the efficiency for tracks that begin further from the beam line. It is noteworthy that the histogram of cos(β) shows that most of the descendants have a momentum that is generally in the same direction as the original stau. Figures 14 and 15 show after the original addition to the default strategy list, when more strategies would be added, the efficiency would remain the same. Because of this, unless the definitions of seed, extend and confirm are adjusted this is the most efficient Seed Tracker can be for reconstructing tracks of particles that originate further from the beam line.

Results on Seed Extend’s ability to reconstruct the tracks of descendants of non-promptly decaying staus will now be presented.

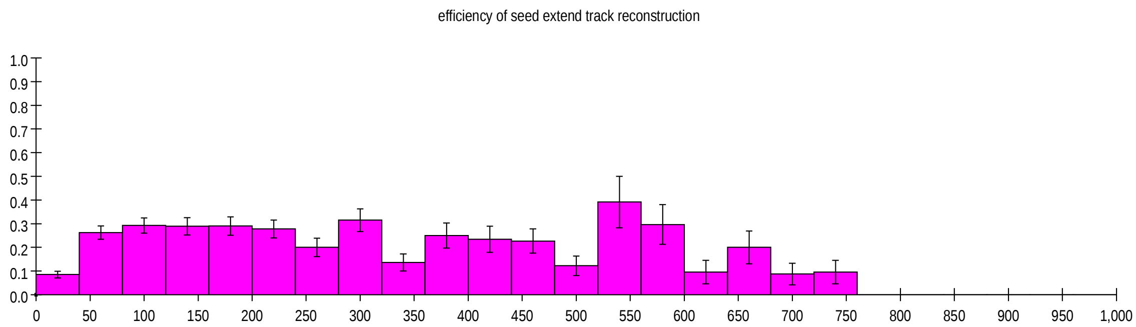

Fig. 16: Original Seed Extend efficiency. This histogram is the original efficiency for reconstructing stau descendant tracks using Seed Extend as a function of the stau descendant radius of origin. The x axis is measured in mm.

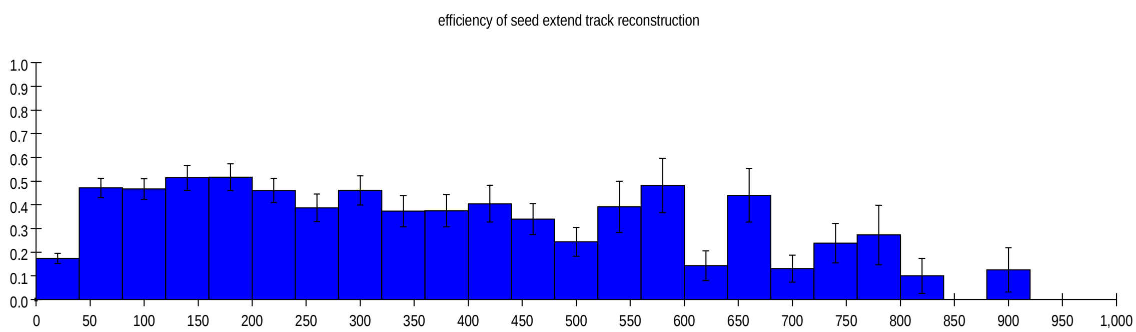

Fig. 17: Efficiency using the modified Seed Extend. This histogram is the efficiency for reconstructing stau descendant tracks using the previously explained modifications to the cuts on Seed Extend as a function of the stau descendant radius of origin. The values on the x axis are in mm.

Figures 16 and 17 show the efficiency of reconstructing stau descendant tracks using Seed Extend as a function of radius of origin before and after all the Seed Extend cuts were modified. From these figures it is obvious that the new cuts gave a better overall efficiency for finding particles using Seed Extend. However by relaxing the cuts more fake tracks are allowed to be considered real. Tables 1 and 2 compare the number of real tracks found with the number of fake tracks made.

	Using Previous Settings	
Radial Range	218-468	468-718
Findable Stau Descendants	400	204
Good Seeds	347	118

Reconstructed Tracks of Descendants (percent)	94 (23.5%)	30 (14.7%)

Tbl. 1: Previous Seed Extend Efficiency. This table provides the data for the original cuts on Seed Extend for particles that begin in the windows of highest track reconstruction efficiency (218-468mm and 468-718mm radius of origin). This separates the number of known findable descendants, then the number of findable stau descendants with reconstructed seeds (good seeds), and the number of reconstructed tracks of findable stau descendants.

	Using New Settings	
Radial Range	218-468	468-718
Findable Stau Descendants	400	204
Good Seeds	351	138
Reconstructed Tracks of Descendants (percent)	168 (42%)	65 (31.9%)

Tbl. 2: Updated Seed Extend Efficiency. This table provides the data for Seed Extend for particles that begin in the windows of highest track reconstruction efficiency (218-468mm and 468-718mm radius of origin) after the previously explained cuts were made. This separates the number of known findable descendants, then the number of findable stau descendants with reconstructed seeds (good seeds), and the number of reconstructed tracks of findable stau descendants.

Comparing Tbl. 1 and 2 it is obvious that the modifications increased the tracking efficiency of the two efficient windows of stau descendant radial origin. However, there is a large increase in the number of fake tracks. Previously only 21 fake tracks were made, however with the new cuts, 40 fake tracks are made. This signifies that the cuts made could have been too relaxed. If this is true then the efficiency for reconstructing tracks using Seed Extend can never be very high.

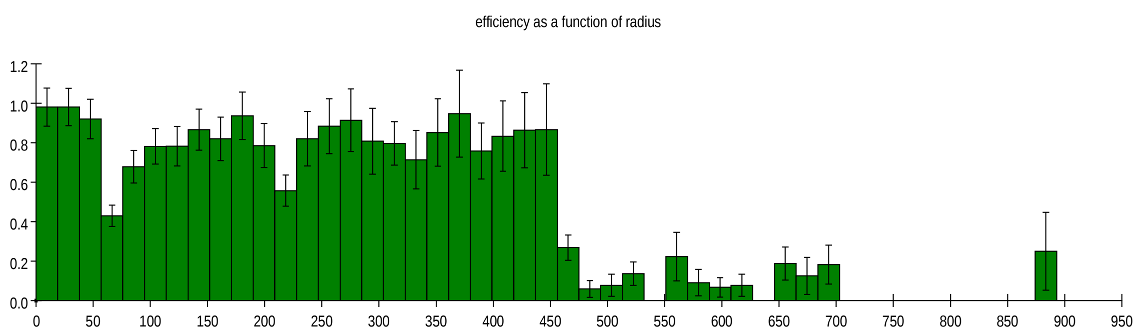

Fig. 18: Original efficiency of all three tracking methods. This histogram shows efficiency for reconstructing tracks of stau descendants using all three original tracking methods as a function of radius of origin. The values on the x axis are in mm.

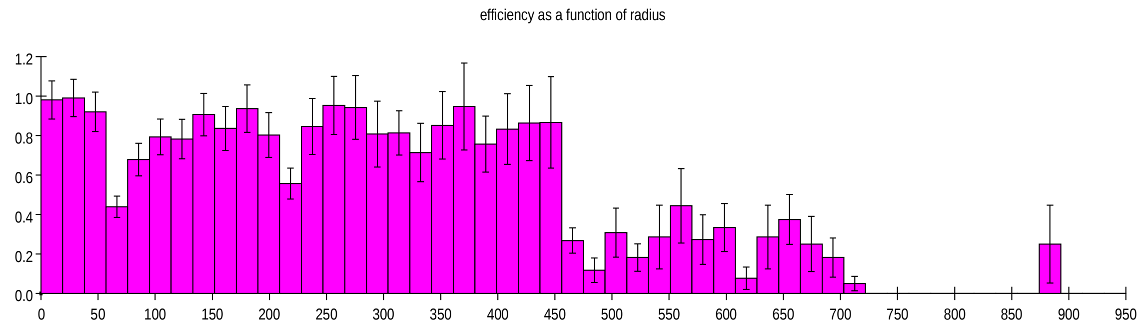

Fig. 19: Overall efficiency using the modified tracking methods. This histogram shows the overall efficiency for reconstructing tracks of stau descendants using the modified Seed Tracker and Seed Extend as well as Garfield Tracker as a function of radius of origin. The values on the x axis are in mm.

Finally, by using all three tracking methods, the overall efficiency for tracking staus increased from Fig. 18 to Fig. 19. Although it increased the number of fake tracks, the modifications to Seed Extend increased the efficiency for tracks that begin further out. The efficiency of reconstructing tracks that begin at higher radii is still low compared to the efficiency of reconstructing tracks that begin at lower radii. Therefore, in order to competently reconstruct tracks that begin at higher radii, work still needs to be done on Seed Extend to improve its efficiency. There is an obvious dip in the efficiency at around 60-90mm radius of origin. This region is too far from the origin for Seed Tracker to be efficient but too close to the origin for Garfield Tracker and Seed Extend to be efficient.

CONCLUSION:

The SiD does show that it can produce fairly good reconstruction efficiency. Seed Tracker does well for reconstructing the prompt tracks and Garfield Tracker does well at reconstructing the non-prompt tracks. Seed Extend has proven that it is difficult to show good efficiency without reconstructing fake tracks. A reason for why Seed Extend is not as efficient as one would hope is because not all the stau descendants that create a seed will have an associated stub.

It was originally hoped that Seed Extend could find many tracks that Garfield Tracker could not, however at the moment this is uncertain. Using the changes on Seed Tracker and Seed Extend it is now possible to analyze stau decays and better create algorithms for precisely finding the point of the decay. There is more work that will be done to increase Seed Extend's efficiency for finding tracks. Backgrounds from other standard processes (such at $e^+e^- \rightarrow e^+e^-$) will need to be considered in order to obtain a clearer picture of how the algorithm is performing. The programs that were created for analyzing the tracking methods will be useful to compare the reconstructed tracks with the known tracks in the future.

If supersymmetry is real it will likely be found at the LHC. If it exists at energies within the reach of the ILC, the precision of the ILC will help to probe the methods of supersymmetry breaking. Furthermore, if GMSB is the method for supersymmetry breaking, the tracks of the descendants of the promptly decaying staus will likely be reconstructed. If the stau does not promptly decay there is a reasonable probability that the tracks of the stau descendants will be reconstructed.

REFERENCES:

1. “The Project” International Linear Collider. 2010. 23 May 2010 <http://www.linearcollider.org/about/What-is-the-ILC/The-project>
2. Aihera, H., Burrows, P.,Oreglia, M. SiD Letter of Intent 31 March 2009
3. Drobychev, G., Fedorov, A., Korjik, M., O. Missevitch. Letter of Intent from the Fourth Detector (“4th”) Collaboration at the International Linear Collider 31 March 2009
4. Graf, N.. sid02 10 Feb. 2009 <https://confluence.slac.stanford.edu/display/ilc/sid02>
5. Gunion, J.F., Haber, H.E. Low-Energy Supersymmetry at Future Colliders December 1997 <http://arxiv.org/PS_cache/hep-ph/pdf/9806/9806330v1.pdf>
6. S. P. Martin. A Supersymmetry Primer December 2008 <http://arxiv.org/PS_cache/hep-ph/pdf/9709/9709356v5.pdf>
7. Schumm, B. “Thoughts About (Silicon) Tracking for the Linear Collider Detector(s).” 10 May 2005. 15 Dec. 2009. <http://scipp.ucsc.edu/~schumm/talks/Davis_05.ppt#7>
8. Stevens, L. Using Monte Carlo Simulation and Longitudinal Segmentation Algorithm in an Attempt to Improve Non-Prompt Track Reconstruction 21 March, 2008. UCSC Thesis

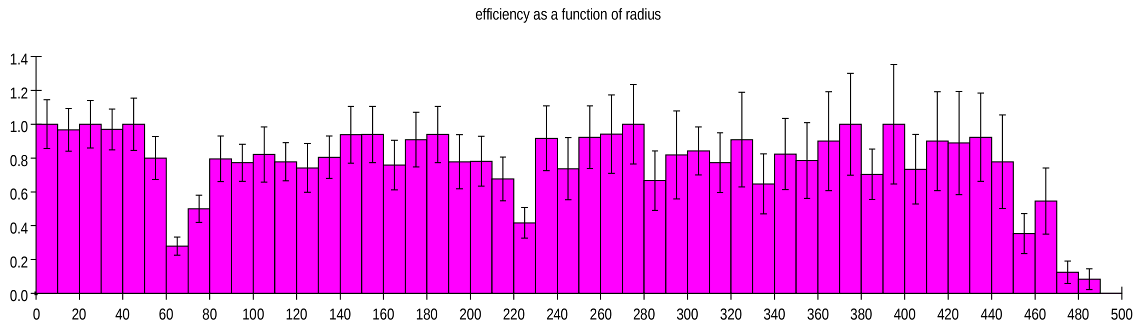
efficiency as a function of radius
0.0 0.2 0.4 0.6 0.8 1.0 1.2 1.4
0 20 40 60 80 100 120 140 160 180 200 220 240 260 280 300 320 340 360 380 400 420 440 460 480 500

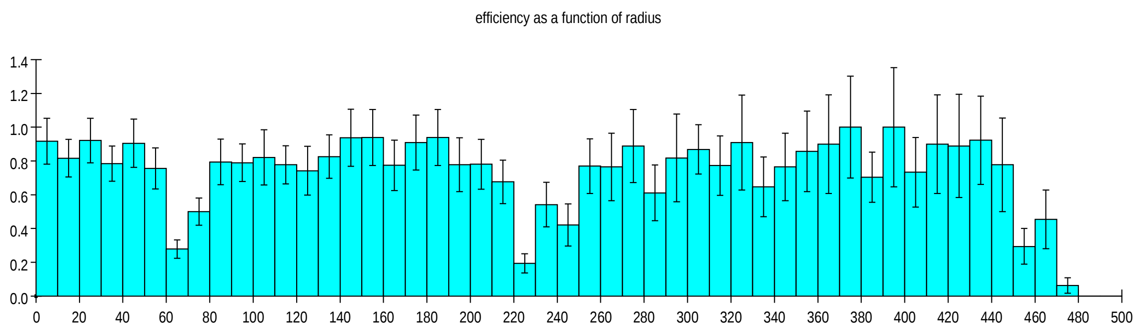
efficiency as a function of radius
0.0 0.2 0.4 0.6 0.8 1.0 1.2 1.4
0 20 40 60 80 100 120 140 160 180 200 220 240 260 280 300 320 340 360 380 400 420 440 460 480 500

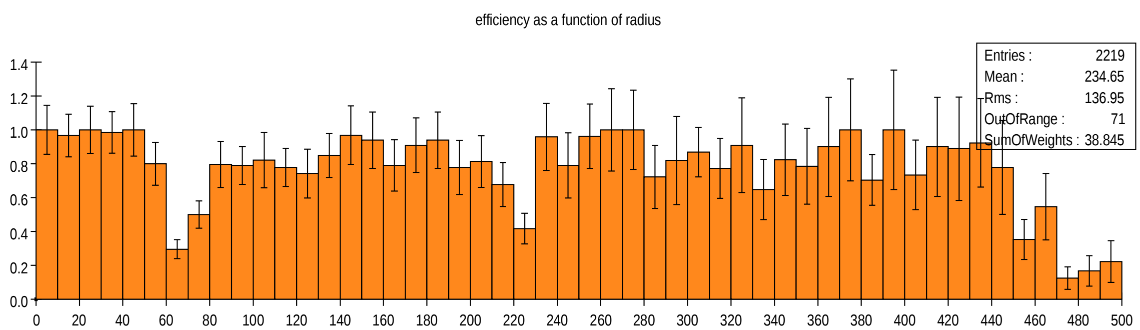
efficiency as a function of radius
Entries : 2219
Mean : 234.65
Rms : 136.95
OutOfRange : 71
SumOfWeights : 38.845
0.0 0.2 0.4 0.6 0.8 1.0 1.2 1.4
0 20 40 60 80 100 120 140 160 180 200 220 240 260 280 300 320 340 360 380 400 420 440 460 480 500